CASE HISTORIES

# Vemurafenib: the first drug approved for *BRAF*-mutant cancer

*Gideon Bollag, James Tsai, Jiazhong Zhang, Chao Zhang, Prabha Ibrahim, Keith Nolop and Peter Hirth*

Abstract | The identification of driver oncogenes has provided important targets for drugs that can change the landscape of cancer therapies. One such example is the *BRAF* oncogene, which is found in about half of all melanomas as well as several other cancers. As a druggable kinase, oncogenic BRAF has become a crucial target of small-molecule drug discovery efforts. Following a rapid clinical development path, vemurafenib (Zelboraf; Plexxikon/Roche) was approved for the treatment of *BRAF*-mutated metastatic melanoma in the United States in August 2011 and the European Union in February 2012. This Review describes the underlying biology of BRAF, the technology used to identify vemurafenib and its clinical development milestones, along with future prospects based on lessons learned during its development.

RAF serine/threonine kinases are important signalling integrators and their founding member *RAF* was identified as a viral oncogene almost 30 years ago[1]. As an oncogene, *RAF* was thus implicated as a driver of cancer cell proliferation. Cloning of the human homologue, *CRAF*[2,3], led to the subsequent realization that two additional homologues existed in the human genome, namely *ARAF*[4,5] and *BRAF*[6,7]. As described below, the RAF kinases have important roles in growth factor signalling pathways (FIG. 1).

In 2002, a major advance in the understanding of the function of BRAF came from the discovery that the *BRAF* gene was mutated in many different cancers[8]. Specifically, most mutations occur at a single codon, codon 600, replacing valine most typically with glutamic acid (the V600E mutation). This codon is in the activation loop of BRAF, a loop found in most kinases that controls kinase activity; mutations (most commonly the V600E mutation) substantially increase kinase activity to drive the proliferation of cancer cells. This mutation occurs in about half of all melanomas[9] and to varying prevalence in many additional cancers, including colorectal cancer[10], papillary thyroid cancer[11–14], anaplastic thyroid cancer[15], serous ovarian cancer[16], non-small-cell lung cancer[17], gastric cancer[18], cholangiocarcinoma[19], Barrett's oesophageal cancer[20] as well as head and neck cancers[21]. Additional *BRAF*-mutated cancers are still being identified; for example, it was shown that certain populations of hepatocellular carcinoma[22], Langerhan's cell histiocytosis[23], gastrointestinal stromal cell tumours[24], multiple myeloma[25], paediatric astrocytomas (which contain mostly *BRAF* duplications)[26–28], pleomorphic xanthoastrocytomas[29,30] and almost all hairy cell leukaemias harbour *BRAF* mutations[31]. Intriguingly, it was found that $BRAF^{V600E}$ mutations are very frequent in nevi[32] — dysplastic lesions that derive from melanocytes and are quiescent and thus benign[33]. Therefore, additional genetic events are probably required to turn a *BRAF*-mutant cell into a malignant cell.

Preclinical studies to validate mutant BRAF as a target have been reported. Cell culture experiments revealed that proliferation of melanoma and other tumour cell lines could be stimulated by the $BRAF^{V600E}$ oncogene and blocked by genetic ablation of $BRAF^{V600E}$ expression[34–38]. Indeed, dependence on mutant BRAF could also be shown *in vivo* using tumour cell lines in which the $BRAF^{V600E}$ gene could be conditionally suppressed; in some cell lines this suppression resulted in regression of established tumours[39]. More recently, genetically engineered mouse models of $BRAF^{V600E}$-driven tumours have been developed for many key cancer types[40–45].

Before the discovery of the *BRAF* oncogene, CRAF was considered to be an enticing target primarily because of studies in the literature showing that it was an important effector of RAS. Numerous drug discovery efforts targeting CRAF led to a number of preclinical compounds[46]. Sorafenib (Nexavar; Bayer/Onyx), originally discovered as a CRAF inhibitor[47], was approved for the treatment of

*Plexxikon, 91 Bolivar Drive, Berkeley, California 94710, USA. Correspondence to G.B. e-mail: gbollag@plexxikon.com*
doi:10.1038/nrd3847
Published online 12 October 2012

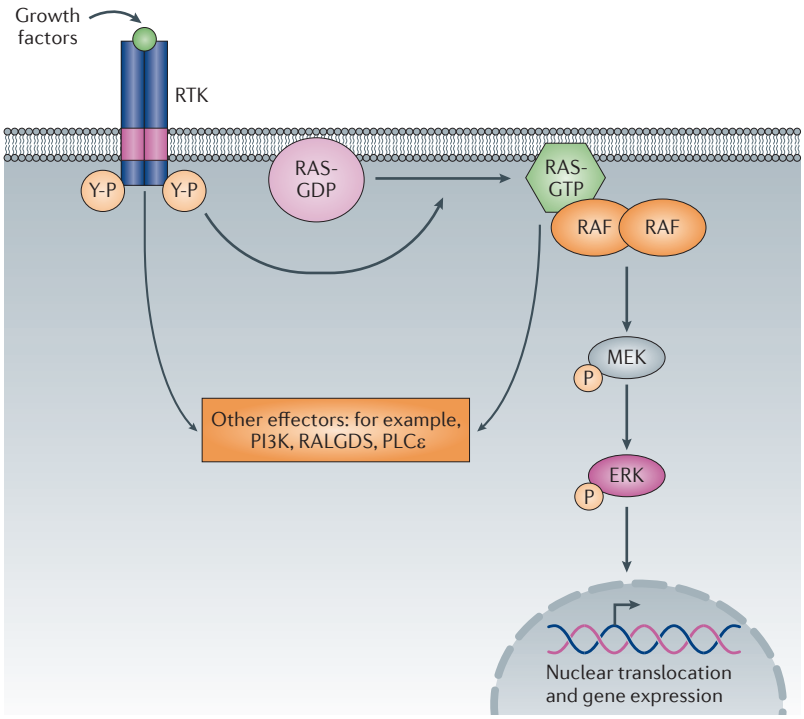


Figure 1 | **The RAF pathway.** Growth factors often bind to receptor tyrosine kinases (RTKs), which are autophosphorylated (illustrated by Y-P) to trigger downstream signalling pathways, including the pathway involving RAS, RAF, extracellular signal-regulated kinase (ERK) and mitogen-activated protein kinase (MAPK)/ERK kinase (MEK). RAF kinase activity initiates a kinase cascade by directly phosphorylating MEK, which in turn phosphorylates ERK to cause translocation of ERK to the nucleus where changes in gene expression take place[132]. Many years after its original identification, RAF was mapped downstream of the *RAS* oncogene[133]. RAS is a molecular switch that cycles between a basal GDP-bound state and an activated GTP-bound state that binds to many different effectors[134]. Demonstration of direct binding between RAS-GTP and RAF[135] led to the finding that membrane-bound RAS-GTP recruits RAF to the membrane[136], generating an active effector kinase. As with many other kinases, RAF family members are regulated by dimerization as well as phosphorylation and dephosphorylation. Dimerization of RAF kinases, which is sometimes induced by the binding of RAS to the kinase, activates the kinase[137]. BRAF–BRAF and CRAF–CRAF homodimerization as well as BRAF–CRAF heterodimerization have been demonstrated[138] (the role of ARAF is not understood in as much detail and so is not discussed here). Feedback phosphorylation events by downstream kinases such as ERK serve in part to disrupt dimers[117]. A related kinase called kinase suppressor of RAS (KSR; not shown in figure) appears to enable this dimerization[90]. PI3K, phosphoinositide 3-kinase; PLCε, phospholipase Cε; RALGDS, RAL guanine nucleotide dissociation stimulator.

renal and hepatocellular carcinoma[48,49]. To date, much of the data suggest that the clinical efficacy of sorafenib derives primarily from its ability to inhibit other kinases such as the vascular endothelial growth factor receptor (VEGFR) family[50]. Sorafenib also inhibits BRAF, but has preference for CRAF and only weakly inhibits $BRAF^{V600E}$. Phase I, Phase II and even large Phase III studies in patients with melanoma did not reveal any clinical efficacy. Patients were not selected for *BRAF* mutations but roughly half of the patients in the trial had melanomas with V600 mutations, so these results raised concerns about BRAF as a cancer target[51–53].

Scaffold
A moderately small molecule — typically 150–350 Da — discovered through screens that measure biochemical activity or in binding assays. Lead optimization of scaffolds usually involves decorating the scaffold with rationally designed substitutions.

Although BRAF was an emerging anticancer target, RAF kinases had been refractory to crystallization for many years, which hampered the identification of selective compounds. With the focus of targeting the RAF family switching to BRAF and the availability of a relatively potent inhibitor in the form of sorafenib, the first crystal structure was finally reported in 2004 (REF. 54). The structural information had important implications for the discovery of vemurafenib (Zelboraf; Plexxikon/Roche), as described below.

Here, we describe the methodology used to discover vemurafenib as well as the preclinical and clinical data that led to its approval for treating *BRAF*-mutant metastatic melanoma. Alongside vemurafenib, a diagnostic test was developed to enable selection of patients. Furthermore, knowledge gained from findings in the clinic and preclinical studies revealed new enigmas of RAF biology, and these are also discussed.

Although the focus of this Review is on the discovery and development of vemurafenib, it should be noted that additional RAF inhibitors are showing promise in clinical trials. The most advanced of these is dabrafenib, which has produced tumour regressions and improved progression-free survival in Phase I–III clinical trials in patients with melanoma[55–57]. Additional compounds include LGX-818, RAF-265 (REF. 58), XL281, ARQ-736 and CEP-32496 (REF. 59); these compounds are at earlier stages of clinical development.

## Scaffold-based discovery of kinase inhibitors

Kinase inhibitors were the subject of intensive drug discovery projects at most large pharmaceutical companies through the 1980s and 1990s[60,61]. By the early 2000s, traditional drug discovery efforts using high-throughput screening of very large compound libraries had led to the discovery of several compound classes — such as quinazolines, amino-pyrimidines, oxindoles and bis-aryl ureas — that inhibited kinase activity; however, none of these had the desired properties for inhibiting BRAF. At Plexxikon, we sought to develop a discovery approach that could identify novel scaffolds for kinases (and virtually any other readily crystallizable protein family) in order to explore new chemical space and novel binding modalities. We used this scaffold-based approach to identify novel kinase inhibitors. This approach screened small molecules with selected chemical properties (molecular mass 150–350 Da, fewer than eight hydrogen bond donors and acceptors, few rotatable bonds and relatively high aqueous solubility) in order to maximize the chemical space that is sampled.

This approach started with a library of 'scaffold-like' compounds, enriched for maximum chemical diversity. As these smaller compounds (that is, those with a lower molecular mass) have limited compositional variabilities, a library of 20,000 compounds covers a relatively large swath of chemical space in the specified molecular mass range[62,63]. It should be noted that many other uses of scaffold- or fragment-based drug discovery for identifying inhibitors of kinases and other protein families have also been described in the literature[60,64–66].

Biochemical assays were then developed that had readouts covering a broad dynamic range of signal output and that had minimal sensitivity to the intrinsic compound interference that would normally plague screening at high compound concentrations. Thus, for the kinase family, five different kinases were screened through the library at a concentration of 200 μM. Compounds that inhibited at least three of the five kinases were selected for follow-up studies. This approach of identifying hits that are weak and non-selective would appear to be counter-intuitive to traditional drug discovery methods. Furthermore, it would be anticipated that a screen at such high concentrations might be prone to false positives. These issues were addressed at the very next step of the approach: co-crystallography. A co-crystal structure of the kinase and the hit compound unambiguously identified true binding interactions. Using this approach, new compound classes were readily identified.

From the initial screen, 238 compounds were selected for co-crystal analysis: the compounds were mixed with crystallography-grade, recombinant kinase domains from the various kinases that the compounds bound in buffers favouring crystal growth. For those compounds that yielded co-crystals in one of several kinase crystallization systems, three-dimensional structures were determined. Eventually, over 100 structures of kinases co-crystallized with bound compounds were successfully determined. In particular, the serine/threonine kinase PIM1 provided a robust system to identify novel scaffold candidates[67]; initially, PIM1 and a second kinase, fibroblast growth factor receptor 1 (FGFR1), provided more reliable crystallization systems while BRAF crystallization conditions were in optimization.

The three-dimensional structural analysis revealed atomic-level detail of the binding interactions despite the weak affinity of these initial hits. The co-crystal structures also confirmed that compounds identified as hits in the original screening did indeed bind the target kinase. With the structural information at hand, chemists, computational chemists and structural biologists could select the best screening hits and rationally design a next iteration of compounds for synthesis. Important criteria for scaffold selection included the number of sites for substitution by chemical groups, the orientations of the substitution sites in the binding pocket and differentiation of the hits from the known chemical space.

Based on this approach, a 3-substituted 7-azaindole was selected for further optimization based on the structure of the compound co-crystallized with PIM1 (REF. 62) (FIG. 2). Synthetic chemistry coupled with additional co-crystallography, this time with FGFR1, yielded a substantial improvement in the affinity of the compound for the kinase, which was due to an increased number of binding interactions. Subsequent optimization required development of a BRAF structure analysis.

In order to generate a robust expression and crystallization system for BRAF, a highly soluble form of the truncated kinase domain was engineered by mutating surface hydrophobic residues into relatively isosteric hydrophilic amino acids[62]. Using this approach, we were able to determine the co-crystal structures of over 100 different compounds bound to BRAF. Once iterations of co-crystallography, computational simulation, chemistry and biological assays were adapted to the BRAF system, progress towards identifying potent, selective compounds was very rapid. Vemurafenib and PLX4720 (a sister compound to vemurafenib that had better pharmacokinetics in rodents) were identified within a year of initiating BRAF-specific improvements; these compounds were optimized for binding affinity, selectivity and pharmacokinetic properties.

Although not covered in this article, the scaffold-based drug discovery paradigm outlined above can be readily applied to other protein families. Detailed descriptions of efforts to identify phosphodiesterase inhibitors and pan-agonists for the peroxisome proliferator-activated receptors have been published[68,69].

## Biological characterization of vemurafenib

Vemurafenib was first synthesized in early 2005. Initial biochemical characterization of this compound revealed that it has mild selectivity for $BRAF^{V600E}$ over the wild-type enzyme. This indicated a pattern that was noted in the full chemical series, including PLX4720. Structural characterization of the series suggested that there was a straightforward explanation for the selectivity of the compounds for $BRAF^{V600E}$: these compounds bind selectively to the active (known as 'DFG-in'; stabilized by E600) versus inactive form of the kinase[62,70]. The details of this structural interpretation are discussed below in the section on structural binding.

Although selectivity for $BRAF^{V600E}$ over wild-type BRAF in the biochemical assays was modest, selectivity for $BRAF^{V600E}$ over wild-type BRAF in melanoma or colorectal cancer cell lines was remarkable. The reason for this pronounced cellular selectivity was foreshadowed in part by a breakthrough study showing that *BRAF*-mutant cells were highly sensitive to MEK (mitogen-activated protein kinase (MAPK)/extracellular signal-regulated kinase (ERK) kinase; also known as MAPKK) inhibitors; the study determined that when BRAF is the driver of proliferation, the MAPK pathway is essential for cell proliferation[71]. Although both vemurafenib and MEK inhibitors inhibit cellular proliferation, the compounds have different pharmacodynamic effects: MEK inhibitors block ERK phosphorylation regardless of cellular genotype, whereas vemurafenib only blocks ERK phosphorylation in *BRAF*-mutant cells. Indeed, ERK phosphorylation is actually stimulated by vemurafenib in some wild-type *BRAF* cells, and this so-called RAF inhibitor paradox is discussed below in the section describing new RAF biology.

Although there were quantitative differences in the effects of vemurafenib on cell lines derived from different tissues of origin, vemurafenib is generally effective in cells with *BRAF* mutations at codon 600. Thus, the proliferation of $BRAF^{V600E}$ melanoma[72–78], colorectal cancer[73,75,78] and papillary thyroid cancer[79,80] cell lines is inhibited by vemurafenib. A small subset of cell lines from each of these cancer types is inherently resistant to vemurafenib, and the mechanisms of this inherent resistance are now

Chemical space
The potential chemical diversity that is spanned by all possible combinations of atomic elements to yield all possible compounds encompassing all sizes and with all potential chemical and physical properties.

Fragment
A very small molecule — typically less than 250 Da — discovered through biophysical screening methods such as nuclear magnetic resonance (NMR) or X-ray technologies. Often, several fragments that represent discrete binding components will be linked together to enhance potency during lead optimization.

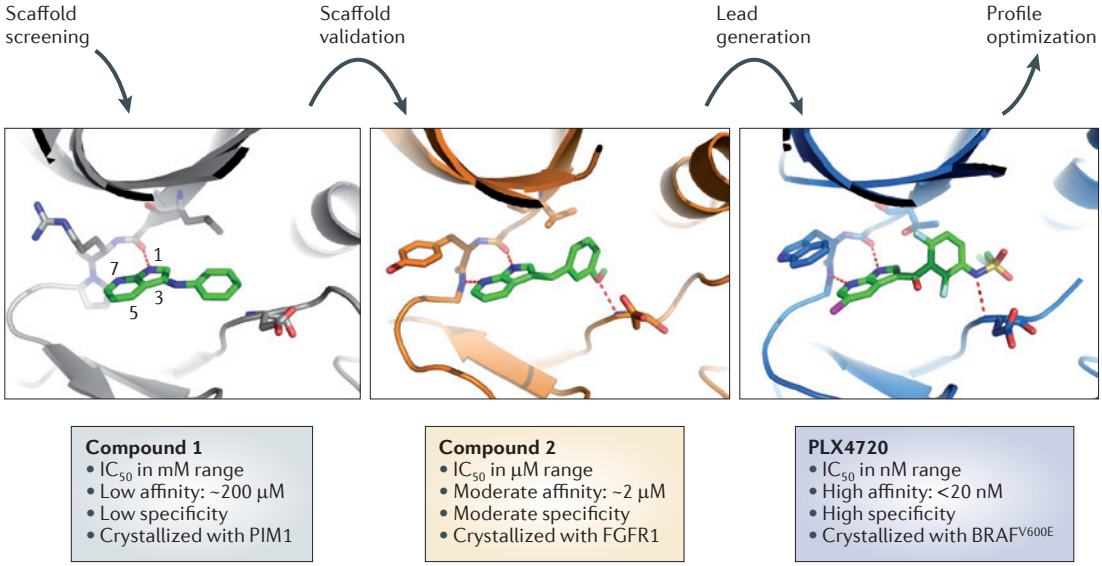


Figure 2 | **From scaffold to lead compound.** Hits that were identified from screening a library of 'scaffold-like' compounds were co-crystallized with representative kinases. The figure shows the co-structure of the azaindole scaffold (compound 1) with the serine/threonine kinase PIM1. The scaffold was validated by synthesizing a set of 3-substituted compounds guided by the co-structure, which resulted in a more potent azaindole analogue (compound 2); this compound, when co-crystallized with the kinase domain of the fibroblast growth factor receptor 1 (FGFR1), revealed a key hydrogen bond interaction with the DFG (Asp-Phe-Gly) backbone. Further structure-guided optimization resulted in PLX4720, the analogue of vemurafenib, which is shown here in complex with the $BRAF^{V600E}$ protein[62]. $IC_{50}$, half-maximal inhibitory concentration. Images modified, with permission, from REF. 62.

under investigation[81–86]. Some putative mechanisms of both inherent and acquired resistance are described below in the section on mechanisms of resistance. Interestingly, several oncogenic *BRAF* mutations at codons other than codon 600 cause reduction or loss of kinase activity[54,87,88]. Although many of these mutant kinases are sensitive to vemurafenib in purified biochemical assays, the cell lines expressing these non-V600 *BRAF* mutations are generally only modestly sensitive to vemurafenib[78]. Characterization of signalling from some of these non-V600 mutant proteins has revealed that they recruit CRAF to form active heterodimers[54,87]. It is believed that the heterodimeric structure leads to inherent insensitivity to BRAF inhibitors in cells, and this relates closely to the RAF inhibitor paradox.

Nonetheless, when *BRAF*-mutant cell lines that are sensitive to vemurafenib *in vitro* are grown as tumour xenografts *in vivo*, such xenografts are also sensitive to orally delivered vemurafenib[62,70,78,89]. Quantitatively, the xenografts have different responses to vemurafenib, just as the antiproliferative potency of vemurafenib varies somewhat in the cultured cell lines, regardless of the tissue of origin. We chose a modestly sensitive cell line to mimic a typical human tumour, COLO205 colorectal cancer cells bearing the $BRAF^{V600E}$ mutation, to explore the pharmacology of vemurafenib. As shown in FIG. 3, when these cells were used in a xenograft model, increasing oral doses of vemurafenib lead initially to tumour stasis (at exposures of ~100 μM multiplied by hour; ~100 μM•hour) and subsequently to tumour regression (at exposures of ~300 μM•hour or above)[70].

Uptake of $^{18}$F-deoxyglucose is an additional biomarker that can be monitored by positron emission tomography (PET) in live animals. This is a sensitive marker of cancer cell metabolism. Vemurafenib can block the uptake of $^{18}$F-deoxyglucose within 1 week of dosing, at drug exposures that correlate with *in vivo* tumour stasis[70].

## Structural analysis of vemurafenib binding

Co-crystallization studies enabled the analysis of information regarding the binding of vemurafenib. Co-crystallization of the $BRAF^{V600E}$ protein with vemurafenib revealed that BRAF forms a dimer (FIG. 4a). As typical of kinase domains, each BRAF protomer contains two different-sized lobes linked by a hinge region and a neighbouring cleft that forms the ATP-binding pocket. Both protomers adopt the so-called 'DFG-in' conformation in which the phenylalanine side chain of the DFG motif in the activation loop is buried inside and away from the ATP-binding pocket, but vemurafenib is present in the ATP-binding pocket of only one of the protomers. In the co-structure of wild-type BRAF with the vemurafenib analogue PLX4720 (REF. 62), the compound bound to one of the protomers with 100% occupancy and the other protomer with 60% occupancy, and the protomer with partial ligand occupancy adopted the 'DFG-out' conformation in which the outward-facing phenylalanine residue obstructed ATP binding. The structural differences between wild-type and mutant BRAF revealed the underlying mechanism for oncogenic activation of BRAF caused by the V600E mutation. In the mutated form of BRAF, the salt bridge formed between Glu600 and Lys507

DFG motif
A motif (Asp-Phe-Gly) that marks the beginning of the activation loop and can assume one of two conformations based on the side-chain orientation of the central residue in the motif: 'DFG-in' and 'DFG-out'. The conformation of the DFG motif affects ATP substrate binding and the catalytic competency of the kinase.

Anchor and grow
A key design strategy of scaffold-based drug discovery, in which the scaffold serves as the anchor that remains constant throughout chemical exploration, and multiple analogues are synthesized systematically by adding substituents to branch points to access unoccupied sub-sites of the drug target.

αC helix
A structurally conserved helix that is present in one of the two lobes that flank the ATP-binding site of a protein kinase. Its conformation is crucial for ATP binding and kinase activity.

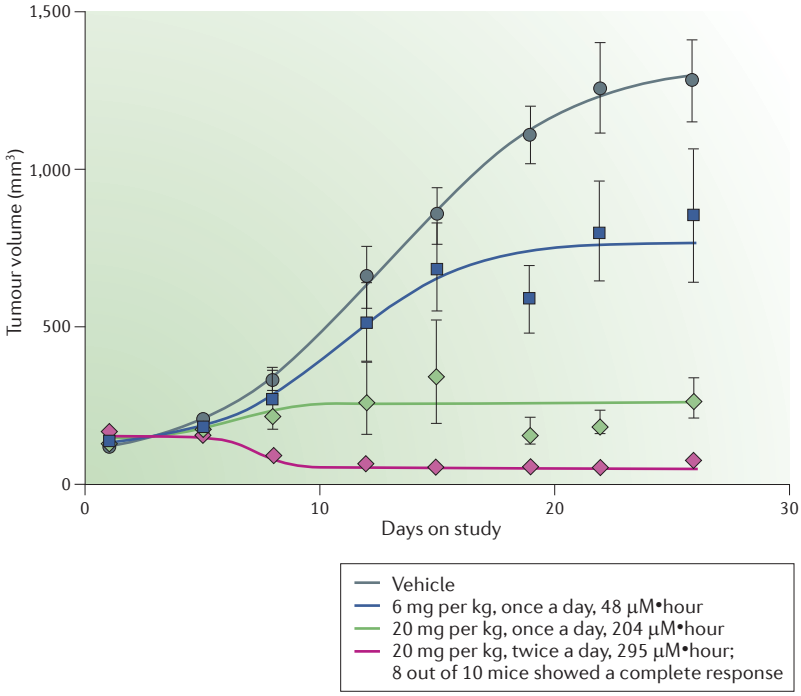


Figure 3 | **Vemurafenib in xenograft models.** The *BRAF*$^{V600E}$-mutant human colorectal cancer cell line was grown on the flank of immunocompromised mice[70]. Mice that had a tumour volume of ~150 mm$^3$ were treated with one of three doses of vemurafenib (or vehicle) given by oral gavage for 4 weeks. A dose-dependent reduction in tumour growth was evident, and pharmacokinetic evaluation was performed at each of the three doses; the day 7 area under the curve (AUC) is provided in the graph. Tumour regression occurred at exposures of vemurafenib of ~300 μM multiplied by hour (~300 μM•hour), and this result established a preclinical threshold of drug exposure to target in clinical trials. Graph reproduced, with permission, from REF. 70 © (2010) Macmillan Publishers Ltd. All rights reserved.

Investigational new drug application
A detailed report of compound characteristics, including synthetic and analytical methods, formulation, pharmacology and toxicology data and clinical plans, that is submitted to the US Food and Drug Administration to request approval to begin clinical testing.

Microprecipitated bulk powder
A stabilized formulation of vemurafenib consisting of amorphous (non-crystalline) microparticles that were prepared by precipitating vemurafenib into a polymer matrix; this process substantially improved the systemic absorption of vemurafenib.

Area under the curve
(AUC). A pharmacokinetic parameter that measures the integrated area under the plasma drug concentration curve as a function of time.

keeps the activation loop in the 'DFG-in' conformation and renders the mutant protein constitutively active.

Co-crystallography had an important role in the discovery of vemurafenib, allowing the application of the modular 'anchor and grow' philosophy of the scaffold-based approach to drug design (FIG. 4b). The 7-azaindole scaffold of the series of lead compounds, identified through a scaffold-based discovery campaign as described above, occupied the hydrophobic cleft next to the hinge region of BRAF kinase, which was maintained as the anchor throughout chemical exploration. The aryl-sulphonamide moiety was discovered after a focused drug design effort to find substitutions that interacted optimally with the backbone amide of Asp594. The propyl tail group was selected because it fit an interior pocket specific to the mutant BRAF protein that was first revealed by the co-crystal structures of the shorter-chain methyl and ethyl analogues. Because the 5-substitution was on a distant site of the azaindole group, the chloro-phenyl group resulted from an independent optimization for improved potency and pharmaceutical properties. The 'anchor and grow' approach enabled the identification of a new generation of kinase inhibitors that selectively target an oncogenic mutation, and it also introduced a new chemical class of kinase inhibitor to be used as a tool compound.

Further structural analysis revealed that the BRAF$^{V600E}$ dimer has an extensive interface between the two protomers, burying ~1,200 Å$^2$ of solvent-accessible surface area on each protomer. Rather than having simple shape complementarity, the interface is dominated by specific polar interactions (including 16 hydrogen bonds and 7 salt bridges)[62,70]. In particular, Arg509 on one molecule forms four hydrogen bonds with the carboxyl terminus of the regulatory αC helix of its dimer partner, and mutation of this residue abolishes dimer formation[90,91]. Although the role of RAF dimerization in regulating kinase activity had been previously recognized, its importance in developing RAF inhibition-based therapy is only now becoming appreciated. The efficacy of a BRAF inhibitor against *BRAF*-driven tumours may depend to a large degree on the effect of the inhibitor on the conformation of the kinase. Unlike previous RAF inhibitors such as sorafenib[54], vemurafenib binding causes an outward shift in the regulatory αC helix (FIG. 4a) of BRAF$^{V600E}$, thereby altering its interaction with Arg509 and in turn affecting RAF dimerization. Although the conformational change, including the shift in the αC helix, induced by vemurafenib is sufficient to block RAF signalling in *BRAF*-mutant cells, this induced conformation does not block the activity of dimeric RAF, and so the drug paradoxically activates the MAPK pathway in cells in which growth is driven by RAS (or other upstream signals). Therefore, at Plexxikon our focus for discovering the next generation of BRAF inhibitors is to find conformation-specific inhibitors that abolish paradoxical activation of MAPK.

## Clinical pharmacology

Before the initiation of clinical studies, work began on the development of a companion diagnostic assay to identify melanomas that harboured the *BRAF* oncogene (BOX 1).

Once vemurafenib was chosen as the clinical development candidate because of its favourable potency, selectivity and pharmaceutical properties, a series of preclinical studies were conducted to predict its safety and pharmacokinetics in humans. Based on these successful toxicology and safety pharmacology studies, an investigational new drug application was filed with the US Food and Drug Administration (FDA) in the autumn of 2006. Almost concurrently, Plexxikon signed a collaboration agreement with Roche Pharmaceuticals to work together to guide vemurafenib through clinical trials.

***Reformulation studies.*** The initial formulation of vemurafenib consisted of a crystalline powder (that was stabilized with several common pharmaceutical excipients to aid bioavailability) that was filled into capsules that could be delivered orally[92]. Although this was adequate to initiate clinical testing, it was challenging to manufacture and store, as the crystal form that demonstrated highest solubility was unstable. In order to improve solubility and stability, Roche reformulated vemurafenib into an amorphous material known as a microprecipitated bulk powder[78]. Based on a pharmacokinetic study in healthy volunteers, the microprecipitated bulk powder formulation was shown to result in a sixfold increase in bioavailability compared to the crystalline formulation[92].

***Phase I dose escalation.*** A dose-escalation Phase I safety trial (ClinicalTrials.gov identifier: NCT00405587) using the crystalline powder formulation was initiated in patients with solid tumours at a number of academic hospitals. The first patient was enrolled in November 2006 at a starting dose level of 200 mg per day. No dose-limiting toxicities were observed in the first three patients so the next cohort was started at 400 mg per day. Notably, the elimination half-life observed in the clinic was much slower than predicted from preclinical scaling analyses. A once-daily dosing regimen was possible, but all cohorts of patients (after the first cohort) used a twice-daily regimen to reduce the capsule load per dosing administration. The dose escalations continued in doubling increments without any toxicity. Patients were dosed with increasing numbers of capsules up to the large drug burden of 1,600 mg twice each day, continually until disease progression or adverse events were noted. During the dose-escalation phase, patients were not required to have *BRAF*-mutation-positive tumours to be enrolled in the study. As shown in FIG. 5, the pharmacokinetic studies revealed that drug exposure with the initial formulation resulted in a plateau when patient blood levels reached ~200 μM•hour, which was below the desired threshold of 300 μM•hour that was associated with tumour regression in preclinical studies[92].

However, the reformulation of vemurafenib enabled dose-escalation studies to restart, beginning at one-tenth of the dose level (that is, 160 mg twice per day) of the previous formulation (1,600 mg twice per day). Additional clinical study centres (a total of six) were recruited in order to expedite patient enrolment, especially of patients from whom paired biopsy samples (that is, before and during treatment) could be obtained. As we had confidence in the scalability of the new formulation, we predicted that the next dose level of 240 mg twice per day would cross the threshold of 300 μM•hour and lead to our first evidence of tumour shrinkage in patients in whom a *BRAF* mutation was driving tumour growth. And we turned out to be correct (FIG. 5), providing a beautiful example of translational science from biochemical inhibition via cell-based assays into xenograft models and into the clinic.

Consistent and more pronounced tumour regression, including at metastatic sites such as liver, lung and bone, became commonplace as we continued to escalate the dose of vemurafenib up to 720 mg twice per day. In addition to grade 1 or grade 2 adverse events such as fatigue or rash, the first occurrences of cutaneous squamous cell carcinoma also began to be observed during dose escalation. A dermatology working group was established in order to fully investigate the skin toxicity of vemurafenib, particularly the growth of cutaneous squamous cell carcinomas, which were usually diagnosed as keratoacanthomas that could be easily treated with resection. A rigorous surveillance monitoring plan was also enacted for all ongoing studies. As unacceptable toxicity was documented at the highest dose tested (1,120 mg twice per day), the slightly reduced dose of 960 mg twice per day was chosen for all subsequent clinical studies.

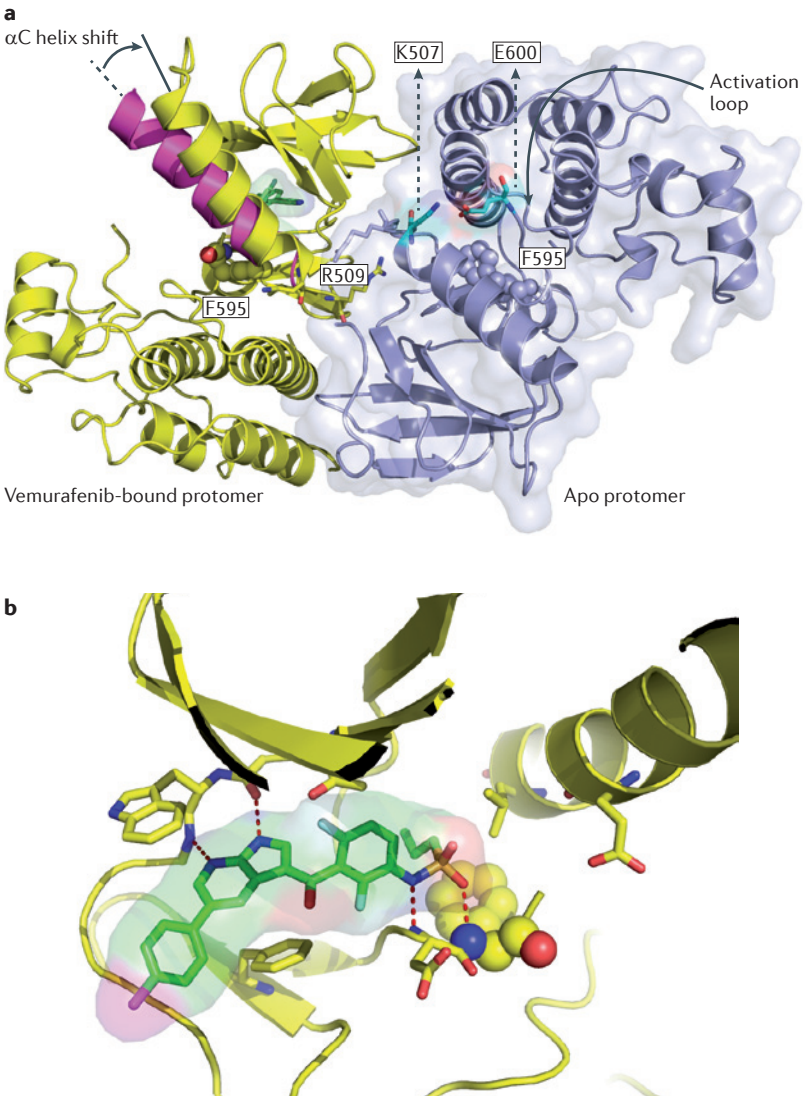


Figure 4 | **Structural studies of vemurafenib.** **a** | The crystal structure of vemurafenib bound to the ATP-binding site of $BRAF^{V600E}$ reveals a dimer that has both protomers in the 'DFG-in' conformation[70]. The interface of the dimer features a key interaction between R509 of one protomer and the carboxyl terminus of the αC helix of the other protomer. Vemurafenib binds to only one protomer (shown in yellow), which causes a movement of the αC helix. This induced fit and conformational selection mechanism underlies the high selectivity of vemurafenib for mutant BRAF kinase. The apo protomer of $BRAF^{V600E}$ (shown in purple) also adopts the 'DFG-in' conformation in part because the V600E mutation stabilizes this conformation through an ionic interaction with K507. By contrast, the apo protomer of wild-type BRAF is only observed in the 'DFG-out' conformation. This explains how a point mutation causes $BRAF^{V600E}$ to become constitutively active. The phenylalanine residue from the DFG loop (F595) is illustrated in sphere representation to highlight the DFG conformations. **b** | The figure shows an enlarged view of vemurafenib in the $BRAF^{V600E}$ active site. Vemurafenib (carbon atoms shown in green, nitrogen atoms shown in blue, oxygen atoms shown in red, fluorine atoms shown in cyan, sulphur atom shown in orange and chlorine atom shown in pink) is illustrated in the bound protomer (shown in yellow). Key hydrogen bond interactions between vemurafenib and active site residues are shown with red dotted lines. Images reproduced, with permission, from REF. 70 © (2010) Macmillan Publishers Ltd. All rights reserved.

## Clinical efficacy and safety

***Clinical studies in patients with melanoma.*** Together with the clinical investigators, we determined that in this Phase I study we had the extraordinary opportunity to provide a clinical benefit for patients with metastatic melanoma,

Box 1 | **BRAF diagnostic development**

Recognizing the importance of accurately determining which melanomas harbour the *BRAF* oncogene, we initiated collaboration with Roche Molecular Systems in 2005 (a year before clinical development of vemurafenib (Zelboraf; Plexxikon/Roche) was initiated).

In order to achieve a robust, reproducible assay, multiple obstacles must be overcome. First, the formalin-fixed paraffin-embedded tissue (FFPET) samples can contain tissue of varying quality and age, and can also contain endogenous inhibitors of DNA polymerases, which can compromise results[129,130]. For melanoma samples in particular, the endogenous melanin can present a problem. Therefore, extraction of DNA from the FFPET samples required considerable optimization. Generation of the PCR reagents and configuration and optimization of the PCR assay also required substantial resources. Furthermore, the logistics to locate the FFPET samples at the clinical trial site (or at the clinic where the patient was initially diagnosed) and transport them to the analytical laboratory, followed by communication of the results to the clinical investigators, were highly time-sensitive considerations.

Scientists from Roche Molecular Systems developed a real-time PCR assay to detect the $BRAF^{V600}$ mutation[129,130]. The assay can detect *BRAF* mutations directly in FFPET samples, allowing the testing of archived samples. This technology involves a complementary primer pair to amplify the *BRAF* sequence surrounding the V600 codon and includes two fluorescently labelled probes. One probe recognizes wild-type DNA sequence (GTG) and the other recognizes mutant DNA sequence (GAG); each probe is labelled with a distinct fluorophore. The probes include both a fluorescent label and a quencher. If the probe properly hybridizes to the DNA sequence, then the nuclease activity of the PCR polymerase would sever the quencher, thereby enabling fluorescence of the hybridizing probe. As both wild-type and mutant probes are included in the same reaction, each detection reaction includes a full in-process control.

The BRAF assay yielded exceptional analytical performance[94,95,130]. Input of 125 ng genomic DNA (obtainable from a 5 μm FFPET section) that contained 5% mutant alleles yielded a >96% hit rate[130]. This was a significantly higher specificity and sensitivity than conventional sequencing would provide. Interestingly, although the assay was designed to specifically detect the V600E mutation, it fortuitously also frequently detects V600K mutations as well as the more rare V600D mutations.

The development of the companion diagnostic assay was synchronized closely to the clinical development of vemurafenib[131].

Following development of the prototype diagnostic assay concurrent with the Phase I trial, the assay was used as an enrolment criterion for the Phase II and Phase III trials[94,95,130]. The clinical samples accessed through the Phase II and Phase III trials also provided validation for the diagnostic assay. Results from the proprietary BRAF assay were compared to conventional Sanger sequencing, and discrepant data were resolved using the more sensitive deep-sequencing method known as 454 sequencing[130]. The aggregate data were submitted to the US regulatory authorities in May 2011, and the diagnostic assay received marketing approval in August 2011, concurrent with the approval of vemurafenib.

so we enrolled 32 patients in the so-called melanoma extension arm at a dose of 960 mg twice per day (ClinicalTrials.gov identifier: NCT00405587). The 81% unconfirmed overall response rate in metastatic melanoma (as illustrated in FIG. 6a) was unprecedented[92]; furthermore, the duration of the tumour response and benefit of prolonged overall survival of patients receiving the 960 mg twice-daily dose was compelling when compared to patients with wild-type *BRAF* or those treated with subtherapeutic doses of vemurafenib. Moreover, on the basis of data obtained from the cohort of patients in the melanoma extension arm of the trial, we and our colleagues at Roche felt confident enough to initiate a well-powered randomized Phase III study concurrent with a Phase II study and other Phase I studies that would be needed for the regulatory registration of the drug.

Elimination half-life
A pharmacokinetic parameter that measures the time it takes for half of a drug concentration to be eliminated from circulating plasma.

Preclinical scaling analyses
Methods for predicting the pharmacokinetic properties of a drug in humans by extrapolating from its pharmacokinetic properties in multiple animal species.

***Studies in patients with colorectal cancer.*** Activating *BRAF* mutations are observed in approximately 10% of patients with metastatic colorectal cancer and are associated with a poor prognosis[10]. Therefore, a cohort of 21 patients with *BRAF*-mutant colorectal cancer was treated at the recommended Phase II dose of 960 mg twice per day (ClinicalTrials.gov identifier: NCT00405587). Although there was unquestionable evidence of activity, including in one patient who had a partial response, it was evident that the biology of *BRAF*-mutant metastatic colorectal cancer was different from that of *BRAF*-mutant melanoma (as illustrated in FIG. 6b)[93]. Future studies in patients with *BRAF*-mutant colorectal cancer will most probably involve combining vemurafenib with other agents.

## Responses in melanoma in a Phase II clinical trial

The objective of the Phase II study was to evaluate the efficacy and safety of vemurafenib in a larger cohort of patients with melanoma who had an activating *BRAF* mutation and had been previously treated with one or more therapies (ClinicalTrials.gov identifier: NCT00949702)[94]. A total of 132 patients were enrolled, including 10 patients with $BRAF^{V600K}$ mutations (the remaining patients had $BRAF^{V600E}$ mutations; see BOX 1). The results of an independent review committee evaluation showed that the confirmed overall response rate was 53%, including 6% of patients with complete responses. The median duration of response was 6.7 months.

Interestingly, some clinical responses were first noted after patients had been taking vemurafenib for over 6 months. Most importantly, as these patients had been followed for over a year, the median overall survival was 15.9 months, which compares favourably with the 6–10 months previously observed in patients with metastatic melanoma. The most common adverse events were grade 1 or grade 2 arthralgia (joint pain), rash, photosensitivity, fatigue and alopecia. Cutaneous squamous cell carcinomas (the majority of which were of the keratoacanthoma type) were diagnosed in 26% of patients. Subsequent work (described below) indicates that these cutaneous lesions probably resulted from paradoxical RAF–MEK–ERK pathway activation in predisposed sun-damaged skin.

## Pivotal Phase III trials

The pivotal Phase III study was a large (675-patient), randomized, controlled study designed to evaluate the efficacy and safety of vemurafenib as a monotherapy compared to dacarbazine in previously untreated patients with unresectable stage IIIc or stage IV melanoma, who were positive for the $BRAF^{V600}$ mutation (BOX 1) (ClinicalTrials.gov identifier: NCT01006980)[95]. The first patient was enrolled in January 2010, and enrolment was rapid. Beginning mid-year, emerging Phase I and Phase II data (as described above) showed substantial clinical activity of vemurafenib in previously treated patients with melanoma, as shown by a confirmed best overall response rate of >50% and median progression-free survival of approximately 7 months[92,94]. By contrast, historical response rates of approximately

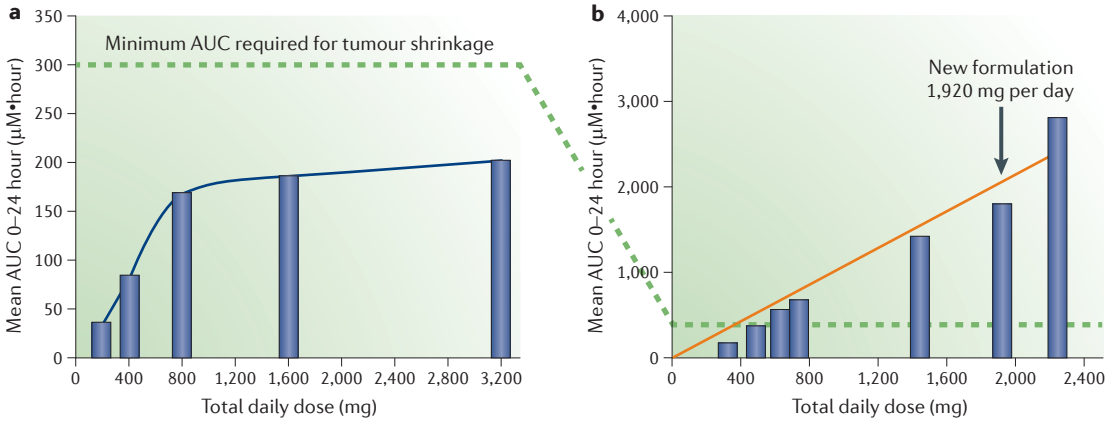


Figure 5 | **Pharmacokinetic analysis of vemurafenib exposure in human plasma.** **a** | The initial crystalline formulation led to saturation of exposure despite very high daily doses. This highlighted the need for a new formulation. The exposure of 300 μM multiplied by hour (300 μM•hour) calculated from preclinical studies (see FIG. 3), which was required to cause tumour regression, is indicated by the dotted line. **b** | Reformulation of vemurafenib as a microprecipitated bulk powder led to a sixfold improvement in plasma levels of the drug without causing apparent saturation[78,92]. AUC, area under the curve.

Adverse events
Adverse side effects graded, by the common toxicity criteria, from 0 (no adverse event) to 5 (fatal adverse event). Grade 1 adverse events are generally mild in severity.

Cutaneous squamous cell carcinoma
Neoplasm of the skin characterized by epithelial cells with a squamous histology.

Keratoacanthoma
A specific low-grade subtype of cutaneous squamous cell carcinoma with a characteristic morphology, believed to originate from the hair follicle.

Unconfirmed overall response rate
The percentage of patients with a partial or complete response recorded from the tumour-imaging scan that showed the highest tumour reduction.

Confirmed overall response rate
The percentage of patients with a partial or complete response who have shown maintenance of tumour reduction using a second tumour-imaging scan taken at least 4 weeks after the initial scan.

Complete response
Determined using RECIST (response evaluation criteria in solid tumours); indicates a 100% reduction in the combined width and length (two-dimensional measurements) of the target lesions of a tumour and no new tumour growth.

Dacarbazine
A chemotherapeutic that kills dividing cells by alkylating DNA and has been approved to treat metastatic melanoma.

Progression-free survival
The duration of time that a patient with cancer survives, in which a tumour does not increase by more than 20% in size.

10% and progression-free survival of approximately 2 months had been observed in previous studies with dacarbazine.

To minimize unnecessary exposure of patients to dacarbazine in the control arm, the FDA recommended that the Phase III statistical analysis plan be revised to assume a greater clinical benefit of vemurafenib. Accordingly, the interim analysis of overall survival rates was significantly moved forward. In mid-January 2011, the data safety and monitoring board of the clinical trials recommended the release of the results of this study owing to the compelling efficacy of vemurafenib. The board also recommended that dacarbazine-treated patients be permitted to receive vemurafenib. Analysis of data from the Phase III clinical trial showed that there was a clinically meaningful and statistically significant improvement in the duration of survival in patients who received vemurafenib compared to those who received dacarbazine ($P$ <0.0001), with a 63% reduction in the risk of death (hazard ratio: 0.37)[95]. Longer follow-up of the patients from the Phase III trial will be necessary to provide reliable estimates of median overall survival.

## Clinical development timeline and lessons learned

The time period of slightly less than 5 years between the filing of the investigational new drug application and its approval by the FDA (in August 2011) included a 6-month suspension in dose escalation owing to the need to reformulate the drug product. Communications with European regulatory agencies were also efficient and approval in Europe was achieved in February 2012. For an oncology indication, this is a very rapid development and approval timeline. Here, we summarize the take-home lessons that we learned from this rapid development of vemurafenib.

Following the initiation of the collaboration between Plexxikon and Roche, Roche decided that Plexxikon should file the initial investigational new drug application and conduct the Phase I clinical trial in order to prevent any time delays resulting from hand-over of responsibilities. This was a wise decision in retrospect, as the stability of the Plexxikon team has provided a solid institutional history for the compound.

Internally, information flow and decision making was efficiently coordinated among Plexxikon, Roche Molecular Systems (which was responsible for the BRAF diagnostic) and Roche Pharmaceuticals (which was also responsible for clinical development), as this was a very fast-moving programme. Starting with the six Phase I clinical sites, the investigators were always engaged and motivated; their enthusiasm spread through the community of investigators as Phase II and Phase III sites were selected. In addition, several teleconferences and face-to-face meetings were held with the FDA and the Committee for Medicinal Products for Human Use of the European Medicines Agency, enabling real-time adjustments (which were supported by the emerging data) to be made to the clinical strategy.

The 'at-risk' initiation of the pivotal Phase III study on the basis of the Phase I extension cohort data required a leap of faith, but this was guided by the remarkable consistency of the cumulative evidence gained from preclinical studies and the results of Phase I clinical trials.

## Clinical pharmacodynamics

During Phase I clinical trials, a subset of patients with melanoma who had accessible tumours had a biopsy procedure twice (known as paired biopsy samples): once before receiving the first dose of vemurafenib and again after 14 days of dosing[70,92]. These biopsy samples were analysed for activation of the BRAF pathway by monitoring ERK phosphorylation (pERK) and also stained for the proliferation marker Ki67. In addition, PET imaging of $^{18}$F-deoxyglucose uptake was monitored before dosing and at day 14 for all patients in the Phase I extension study[96]. The responses of all evaluable patients were documented,

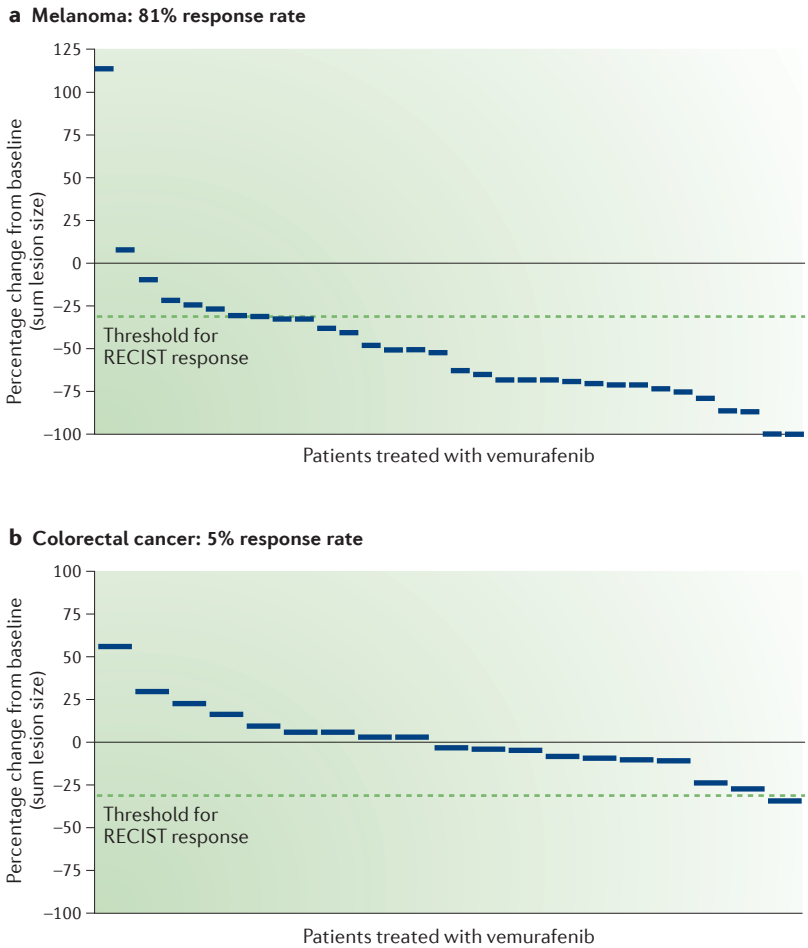


Figure 6 | **Vemurafenib-mediated tumour regression.** The plots show the degree of tumour growth (above 0) or regression (below 0) at the optimal measurement as determined by X-ray computed tomography. The RECIST (response evaluation criteria in solid tumours) criteria stipulate that any regression greater than 30% is scored as a partial response, and this is indicated by the dotted lines. **a** | Vemurafenib produced substantial tumour regression in patients with *BRAF*$^{V600E}$ metastatic melanoma; the unconfirmed response rate in the melanoma cohort was 81%, and the confirmed response rate was 56%[92]. **b** | Patients with *BRAF*$^{V600E}$ colorectal cancer had a much lower response rate than patients with *BRAF*$^{V600E}$ metastatic melanoma.

and examples of the remarkable responses are shown in FIG. 7. Regarding the pharmacodynamic end points of BRAF pathway activation, we initially anticipated that >50% inhibition of the BRAF pathway would produce clinically meaningful results. As discussed below, the results provided an important surprise: tumour regressions were only noted following near-complete inhibition of the pathway.

The first trigger for taking paired biopsy samples was achievement of a measured pharmacokinetic exposure of 100 μM•hour; as shown in FIG. 3, this exposure correlated with tumour stasis in xenograft studies. We were initially encouraged to find that most of the biopsy samples taken at day 14 revealed greater than 50% reduction in pERK and Ki67 staining. However, no tumour regressions were noted and progression-free survival was generally not different from historical controls.

Hazard ratio
A statistical analysis that measures the significance of a clinical end point by comparing the rate of events in two different cohorts: for example, patients who are not exposed and those who are exposed to a new agent. A hazard ratio of 1 means that there is no effect; a hazard ratio of 0.6 implies that the treated cohort has 60% of the hazard of the untreated cohort (that is, the agent reduces the hazard by 40%).

Nonetheless, the reformulated version of vemurafenib led to much higher exposures. Paired biopsy samples taken from patients with these higher drug exposures were quite striking: there was a greater than 80% reduction in both pERK and Ki67 staining. FIGURE 8 compares tumour regression to the pharmacodynamic end point reductions in pERK and Ki67 staining. Corresponding with these higher exposures and substantial pathway inhibition, significant tumour regression was frequently observed in tumours exposed to these higher drug doses[70,92] (FIG. 8).

## New RAF biology revealed by BRAF inhibitors

As the promising clinical results were reported, the Plexxikon compounds were made available to academic investigators who then began to investigate the role of BRAF inhibition in great detail. These academic studies included exploring the mechanism of inhibition in *BRAF*-mutant tumours and describing the mechanisms of resistance to vemurafenib. They also investigated the effects of RAF inhibition in cells that lack *BRAF* mutations. Within the past 2 years, well over 200 manuscripts describing the effects of vemurafenib have been published. Below, we provide a necessarily brief synopsis of these manuscripts.

Many laboratories have confirmed that vemurafenib selectively inhibits the MAPK pathway in several *BRAF*-mutant cancer cell lines originating from melanoma, thyroid and colorectal tumours[44,72–74,76–82,97,98]. The inhibition of proliferation and occasional induction of apoptosis is quite variable from cell line to cell line. Mechanistic studies looking at markers of downstream pathway modulation, apoptosis markers, cell cycle analysis, anchorage-independent growth and transcriptional profiling have revealed important similarities and differences among the cell lines. A link between oncogenic BRAF and activation of metabolic pathways was also reported[99], and studies to investigate combinations of vemurafenib with metabolic modulators are emerging[100]. Studies in zebrafish revealed that the drug interacts with enzymes that control developmental pathways in neural crest cells[101].

***Mechanisms of resistance.*** As melanoma lines have a broad range of differential sensitivity to vemurafenib, the causes of inherent resistance have been addressed in some of the studies. The role of concurrent activation of the phosphoinositide 3-kinase (PI3K) pathway through loss of phosphatase and tensin homolog (PTEN) is clearly important but does not always predict poor sensitivity to vemurafenib[42,72,84,102]. It appears that additional factors besides MAPK and PI3K pathway activation are involved, and future work should reveal these factors. Indeed, one additional factor has been identified: cell cycle control through the retinoblastoma protein tumour suppressor[86].

As discussed above, the therapeutic activity of vemurafenib in patients with *BRAF*$^{V600E}$ colorectal cancer was less impressive than its activity in patients with *BRAF*$^{V600E}$ melanoma. Recently, an important cause of inherent resistance to BRAF inhibition was identified: activation

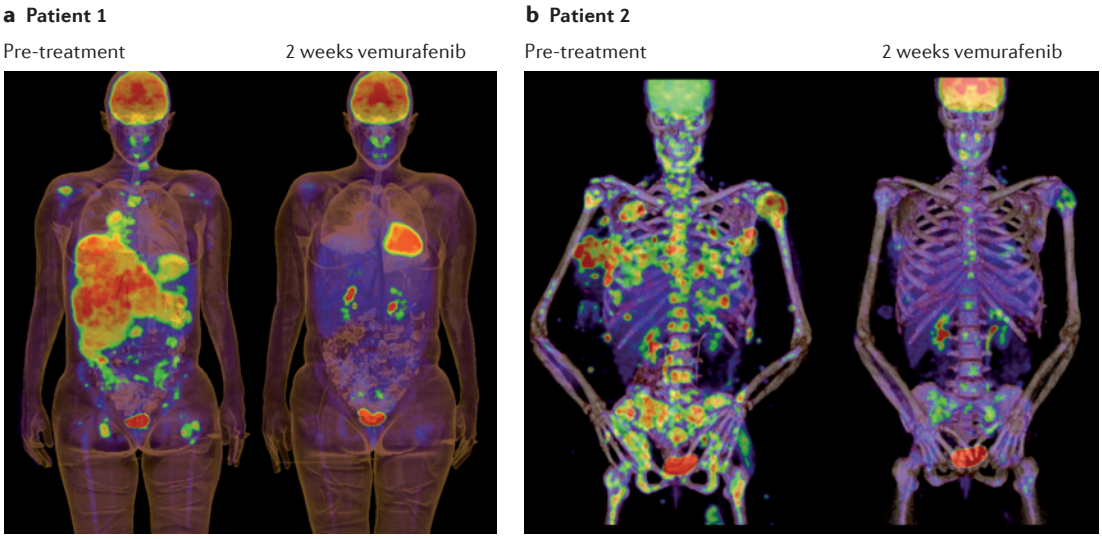


Figure 7 | **PET scans of patients treated with vemurafenib.** Positron emission tomography (PET) scanning was used to visualize uptake of $^{18}$F-deoxyglucose, as shown in two patients (panel **a** and panel **b**) from the Phase I extension cohort[96]. In both panels **a** and **b**, the left image is taken before initiating therapy and the right image is taken after 2 weeks of vemurafenib treatment. All evaluable patients from this cohort experienced reduction of PET signal within 2 weeks. Results from the PET scans showed remarkable blockade of tumour metabolism by vemurafenib. Images courtesy of G. McArthur and R. Hicks, Peter MacCallum Cancer Centre, Melbourne, Australia.

of the epidermal growth factor receptor (EGFR)[103,104]. Thus, combinations of vemurafenib with EGFR antagonists would provide an attractive therapeutic avenue for patients with *BRAF*-mutant colorectal cancer. Perhaps alternative growth factor receptor pathways will have a key role in inherent resistance to BRAF inhibition in other *BRAF*-mutant cancers.

Most patients with melanoma show some degree of tumour regression in response to treatment with vemurafenib, yet relapse often occurs within a year. This suggests that BRAF inhibition can be circumvented with acquired resistance, and many different mechanisms for this resistance have been proposed to date. Perhaps the first mechanism to be proposed involved upregulation of CRAF expression[105]. As elaborated below, this makes considerable sense given the propensity of RAF inhibitors to induce paradoxical activation of the MAPK pathway. However, this has not been extensively documented in clinical specimens from patients who become resistant to vemurafenib.

A second mechanism that has been documented in a number of preclinical and clinical samples involves oncogenic activation of NRAS, an isoform of the *RAS* oncogene that is found in a subset of primary melanomas[106]. Furthermore, upregulation of growth factor receptor pathways such as platelet-derived growth factor receptor (PDGFR)[106] and insulin-like growth factor 1 receptor (IGF1R)[107] pathways has been documented in preclinical and clinical studies. It appears that amplification of the *BRAF* oncogene can also occur[108], and this mechanism has also been suggested for overcoming the effects of MEK inhibitors[109,110]. Recent evidence has also implicated hepatocyte growth factor and its receptor MET as determinants of resistance to vemurafenib[111,112].

Interestingly, in contrast to the most common events mediating resistance against other kinase inhibitors, no second-site mutations in the *BRAF*$^{V600E}$ locus have been found[113]. However, an on-target genetic alteration has been identified in the *BRAF*$^{V600E}$ locus, namely the truncation of the RAS-binding domain of BRAF that results in a constitutively dimerized BRAF$^{V600E}$ protein. This discovery is consistent with the idea that RAF inhibitors are considerably less effective inhibitors of the dimeric enzyme, as described below[114].

***Mechanisms of MAPK activation.*** Paradoxical activation of the MAPK pathway by RAF inhibitors has been referenced many times in this article, so it merits more careful description and consideration. This effect was first reported in 1999 (REF. 115), but it was initially under-appreciated as the available RAF inhibitors did not demonstrate therapeutic utility. Feedback phosphorylation was initially proposed as a key mediator of this effect, and relevant phosphorylation sites were identified[116,117]. However, this feedback is probably only a part of the story[75,118].

Given the clinical success of vemurafenib, the mechanism of paradoxical MAPK pathway activation was revisited in a series of manuscripts published in 2010 (REFS 72,73,76–78,81,88,91,119). These studies show that activation of the MAPK pathway requires activation of upstream growth factor pathways or oncogenic mutation of *RAS*. It is now generally believed that dimerization of the RAF enzyme has a key role in the activation of upstream pathways. Indeed, this had been foreshadowed by important work describing the events involved in RAF dimerization during normal cellular signalling[90]. As mentioned above, RAF dimers are less sensitive to RAF inhibitors, but why does the pathway actually get activated

Neural crest cells
Immature cells found at the crest of the neural plate that give rise to various differentiated cells, including melanocytes.

RECIST
Response evaluation criteria in solid tumours; a set of standardized criteria that define whether patients with cancer have a partial or complete response and stable or progressive disease during treatments.

Partial response
Determined using RECIST (response evaluation criteria in solid tumours); indicates at least 30% reduction in the combined width and length (two-dimensional measurements) of the target lesions of a tumour and no new tumour growth.

On-target genetic alteration
In the context of resistance to a kinase inhibitor, this term refers to a mutation or other genetic alteration in the intended target of the inhibitor that makes the kinase insensitive to the inhibitor.

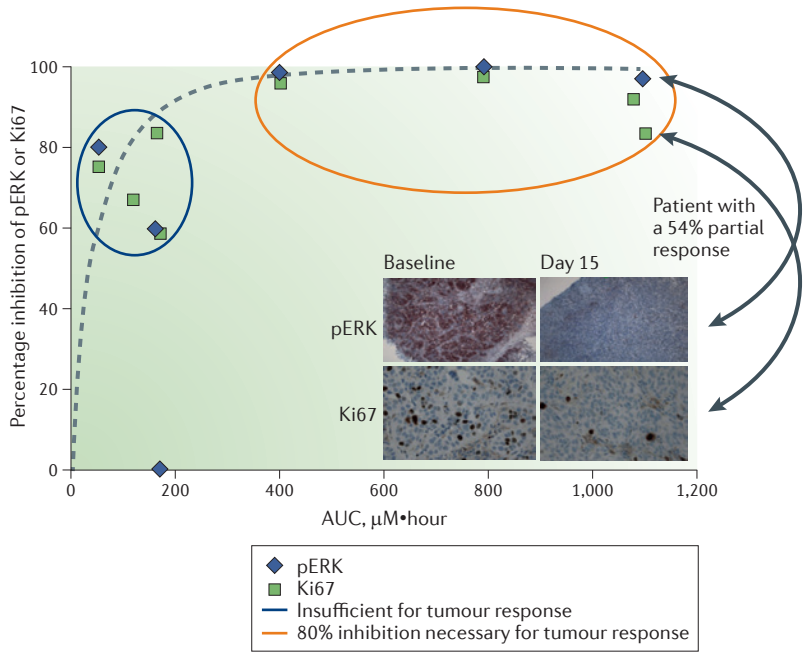


Figure 8 | **Paired biopsy data from a Phase I clinical trial.** Paired biopsy samples from a subset of patients in the Phase I clinical trial were analysed: one biopsy sample was taken before treatment initiation and the second after 2 weeks of vemurafenib treatment[70,92]. Immunohistochemical staining of these biopsy samples was conducted for the presence of two pharmacodynamic parameters, namely extracellular signal-regulated kinase (ERK) phosphorylation (pERK) and the proliferation marker Ki67. The percentage inhibition of these two markers is displayed on the *y*-axis, and the *x*-axis shows plasma levels of vemurafenib. The graph illustrates that even patients with levels of exposure to vemurafenib below 300 μM multiplied by hour (300 μM•hour) have reductions of >50% in the pharmacodynamic parameters. Data circled in blue show patients who did not experience tumour regression. Conversely, data circled in orange indicate patients who did experience tumour regressions. The inset shows representative images of immunohistochemical staining from a patient with 54% tumour regression after 14 days, which was the best response achieved. Overall, these data demonstrate that substantial inhibition of the pathway mediated by BRAF, mitogen-activated protein kinase (MAPK)/ERK kinase (MEK) and ERK is required for tumour regression to occur. AUC, area under the curve. Images reproduced, with permission, from REF. 70 © (2010) Macmillan Publishers Ltd. All rights reserved.

by RAF inhibitors such as vemurafenib? Several related mechanisms have been proposed, including one in which the binding of a RAF inhibitor to one protomer of the RAF dimer allosterically activates the second protomer[91]. It is still unclear whether homodimers or heterodimers of CRAF, BRAF or ARAF kinases are involved, and whether perhaps all dimeric forms can enable paradoxical MAPK activation. Several important studies have also implicated KSR (a protein identified in flies as a kinase suppressor of RAS) in the formation of dimers[90] and in mediating the ability of BRAF to phosphorylate MEK[120]. A role for KSR in mediating paradoxical MAPK activation induced by RAF inhibitors has also been proposed[121,122].

It has been speculated that this RAF inhibitor paradox is responsible for some of the clinical toxicities observed in patients who received vemurafenib; perhaps the most documented example is the development of cutaneous squamous cell carcinomas. Genomic analyses of cutaneous squamous cell carcinoma samples from patients treated with vemurafenib reveal that *HRAS* mutations (another isoform of the *RAS* oncogene) are frequent events in the aetiology of cutaneous squamous cell carcinoma[123,124]. As cutaneous squamous cell carcinomas can appear very quickly after treatment initiation, sometimes within a few weeks of starting vemurafenib, it appears to be likely that there are pre-existing lesions with neoplastic potential in these patients and that vemurafenib (or any conventional RAF inhibitor) accelerates the growth of cutaneous squamous cell carcinomas. Support for this idea comes from preclinical studies in mice, which show that RAF inhibitors do not initiate or promote skin carcinogenesis but substantially enhance proliferation of lesions that have both *HRAS* mutations and are exposed to tumour promoters[123].

## Future directions

The case history of vemurafenib is filled with accounts of revelations, successes and hope. However, despite remarkable tumour regressions and unmistakable improvements in progression-free survival and overall survival, currently very few —if any — patients with metastatic melanoma are cured with vemurafenib. BRAF inhibition, and inhibition of BRAF with vemurafenib in particular, provides an important therapeutic option for patients with metastatic melanoma. One idea that should be explored is the testing of vemurafenib in patients with melanoma that is less advanced, perhaps in the adjuvant setting. Furthermore, studies in other tumours with *BRAF* mutations and combination studies with other therapies are expected. Early studies showed preliminary evidence of vemurafenib activity in patients with thyroid cancer[92]. Recently, anecdotal evidence of efficacy has been reported in a patient with hairy cell leukaemia[125] and in a patient with *BRAF*-mutant lung cancer[126].

As discussed, the activity of vemurafenib as a single agent in *BRAF*-mutant colorectal carcinomas is much less robust than in metastatic melanoma, so combination studies (perhaps with an EGFR inhibitor) could provide a path to improved therapy. Less is known about the activity of vemurafenib in other indications such as papillary thyroid cancer and many of the other cancers mentioned in this article. The coming years should show whether single-agent activity in these other tumours is as remarkable as that seen in metastatic melanoma.

Based on the studies investigating resistance mechanisms and the basic biology of *BRAF*-mutant tumours, many different combinatorial therapies have been proposed. As the MAPK pathway is frequently re-ignited in relapsed tumours, a combination of vemurafenib with a MEK inhibitor is warranted and such studies are underway. Also, the co-dependence of melanomas and other tumours on the PI3K pathway suggests that vemurafenib could be combined with PI3K, AKT or mammalian target of rapamycin (mTOR) inhibitors. There is a rich literature on immunotherapy for melanoma, and one immune-enhancing agent, the cytotoxic T lymphocyte antigen 4 (CTLA4) antibody ipilimumab (Yervoy; Bristol-Myers Squibb), was approved for the treatment of metastatic melanoma in 2011. Studies combining vemurafenib and

Cytotoxic T lymphocyte antigen 4
A receptor on the surface of T cells that mediates downregulation of the immune response.

ipilimumab are underway (ClinicalTrials.gov identifier: NCT01400451), and future combinations with other immunotherapies or vaccines are likely. In this respect, supportive studies have shown that BRAF inhibitors do not blunt the T cell response that is critical for the success of many immunotherapies[127,128].

In parallel with additional clinical trials, knowledge gleaned from the development of vemurafenib has identified areas for improvement in the development of a next-generation BRAF inhibitor. Most notably, the paradoxical activation of MAPK in susceptible cells has been shown to mediate toxicities and may also hamper the durability of the response of a tumour to vemurafenib. Therefore, RAF inhibitors without the propensity to allosterically activate dimeric RAF enzymes are among the next-generation agents under development.

In summary, we believe the case history of the discovery and development of vemurafenib provides a recipe for future personalized medicines. The ingredients include: a driving oncogene; a diagnostic that allows the identification of patients with that oncogene; and a drug that selectively and effectively blocks the function of the oncogene. A future is envisioned in which cancers are first annotated by genetic driving events, and then cocktails of therapeutics that target the key drivers are developed that will be able to cure the patient.


1. Rapp, U. R. *et al.* Structure and biological activity of v-raf, a unique oncogene transduced by a retrovirus. *Proc. Natl Acad. Sci. USA* **80**, 4218–4222 (1983).
2. Bonner, T. *et al.* The human homologs of the raf (mil) oncogene are located on human chromosomes 3 and 4. *Science* **223**, 71–74 (1984).
3. Moelling, K., Heimann, B., Beimling, P., Rapp, U. R. & Sander, T. Serine- and threonine-specific protein kinase activities of purified gag-mil and gag-raf proteins. *Nature* **312**, 558–561 (1984).
4. Huleihel, M. *et al.* Characterization of murine A-raf, a new oncogene related to the v-raf oncogene. *Mol. Cell. Biol.* **6**, 2655–2662 (1986).
5. Beck, T. W., Huleihel, M., Gunnell, M., Bonner, T. I. & Rapp, U. R. The complete coding sequence of the human A-*raf*-1 oncogene and transforming activity of a human A-*raf* carrying retrovirus. *Nucleic Acids Res.* **15**, 595–609 (1987).
6. Ikawa, S. *et al.* B-raf, a new member of the raf family, is activated by DNA rearrangement. *Mol. Cell. Biol.* **8**, 2651–2654 (1988).
7. Marx, M. *et al.* A novel oncogene related to c-mil is transduced in chicken neuroretina cells induced to proliferate by infection with an avian lymphomatosis virus. *EMBO J.* **7**, 3369–3373 (1988).
8. Davies, H. *et al.* Mutations of the *BRAF* gene in human cancer. *Nature* **417**, 949–954 (2002).
**This is a landmark paper that describes the discovery of the *BRAF* oncogene.**
9. Pollock, P. M. & Meltzer, P. S. A genome-based strategy uncovers frequent *BRAF* mutations in melanoma. *Cancer Cell* **2**, 5–7 (2002).
10. Rajagopalan, H. *et al.* Tumorigenesis: RAF/RAS oncogenes and mismatch-repair status. *Nature* **418**, 934 (2002).
11. Cohen, Y. *et al.* *BRAF* mutation in papillary thyroid carcinoma. *J. Natl Cancer Inst.* **95**, 625–627 (2003).
12. Fukushima, T. *et al.* *BRAF* mutations in papillary carcinomas of the thyroid. *Oncogene* **22**, 6455–6457 (2003).
13. Kimura, E. T. *et al.* High prevalence of *BRAF* mutations in thyroid cancer: genetic evidence for constitutive activation of the RET/PTC-RAS-BRAF signaling pathway in papillary thyroid carcinoma. *Cancer Res.* **63**, 1454–1457 (2003).
14. Xu, X., Quiros, R. M., Gattuso, P., Ain, K. B. & Prinz, R. A. High prevalence of *BRAF* gene mutation in papillary thyroid carcinomas and thyroid tumor cell lines. *Cancer Res.* **63**, 4561–4567 (2003).
15. Nikiforova, M. N. *et al.* *BRAF* mutations in thyroid tumors are restricted to papillary carcinomas and anaplastic or poorly differentiated carcinomas arising from papillary carcinomas. *J. Clin. Endocrinol. Metab.* **88**, 5399–5404 (2003).
16. Singer, G. *et al.* Mutations in *BRAF* and *KRAS* characterize the development of low-grade ovarian serous carcinoma. *J. Natl Cancer Inst.* **95**, 484–486 (2003).
17. Brose, M. S. *et al.* *BRAF* and *RAS* mutations in human lung cancer and melanoma. *Cancer Res.* **62**, 6997–7000 (2002).
18. Lee, S. H. *et al.* *BRAF* and *KRAS* mutations in stomach cancer. *Oncogene* **22**, 6942–6945 (2003).
19. Tannapfel, A. *et al.* Mutations of the *BRAF* gene in cholangiocarcinoma but not in hepatocellular carcinoma. *Gut* **52**, 706–712 (2003).
20. Sommerer, F. *et al.* Mutations of *BRAF* and *KRAS2* in the development of Barrett's adenocarcinoma. *Oncogene* **23**, 554–558 (2004).
21. Weber, A. *et al.* Mutations of the *BRAF* gene in squamous cell carcinoma of the head and neck. *Oncogene* **22**, 4757–4759 (2003).
22. Colombino, M. *et al.* *BRAF* and *PIK3CA* genes are somatically mutated in hepatocellular carcinoma among patients from South Italy. *Cell Death Dis.* **3**, e259 (2012).
23. Badalian-Very, G. *et al.* Recurrent *BRAF* mutations in Langerhans cell histiocytosis. *Blood* **116**, 1919–1923 (2010).
24. Agaram, N. P. *et al.* Novel V600E *BRAF* mutations in imatinib-naive and imatinib-resistant gastrointestinal stromal tumors. *Genes Chromosomes Cancer* **47**, 853–859 (2008).
25. Chapman, M. A. *et al.* Initial genome sequencing and analysis of multiple myeloma. *Nature* **471**, 467–472 (2011).
26. Jones, D. T. *et al.* Tandem duplication producing a novel oncogenic *BRAF* fusion gene defines the majority of pilocytic astrocytomas. *Cancer Res.* **68**, 8673–8677 (2008).
27. Pfister, S. *et al.* *BRAF* gene duplication constitutes a mechanism of MAPK pathway activation in low-grade astrocytomas. *J. Clin. Invest.* **118**, 1739–1749 (2008).
28. Sievert, A. J. *et al.* Duplication of 7q34 in pediatric low-grade astrocytomas detected by high-density single-nucleotide polymorphism-based genotype arrays results in a novel *BRAF* fusion gene. *Brain Pathol.* **19**, 449–458 (2009).
29. Dias-Santagata, D. *et al.* *BRAF* V600E mutations are common in pleomorphic xanthoastrocytoma: diagnostic and therapeutic implications. *PLoS ONE* **6**, e17948 (2011).
30. Schindler, G. *et al.* Analysis of *BRAF* V600E mutation in 1,320 nervous system tumors reveals high mutation frequencies in pleomorphic xanthoastrocytoma, ganglioglioma and extra-cerebellar pilocytic astrocytoma. *Acta Neuropathol.* **121**, 397–405 (2011).
31. Tiacci, E. *et al.* *BRAF* mutations in hairy-cell leukemia. *N. Engl. J. Med.* **364**, 2305–2315 (2011).
32. Pollock, P. M. *et al.* High frequency of *BRAF* mutations in nevi. *Nature Genet.* **33**, 19–20 (2003).
33. Michaloglou, C. *et al.* $BRAF^{E600}$-associated senescence-like cell cycle arrest of human naevi. *Nature* **436**, 720–724 (2005).
34. Satyamoorthy, K. *et al.* Constitutive mitogen-activated protein kinase activation in melanoma is mediated by both *BRAF* mutations and autocrine growth factor stimulation. *Cancer Res.* **63**, 756–759 (2003).
35. Tuveson, D. A., Weber, B. L. & Herlyn, M. BRAF as a potential therapeutic target in melanoma and other malignancies. *Cancer Cell* **4**, 95–98 (2003).
36. Karasarides, M. *et al.* B-RAF is a therapeutic target in melanoma. *Oncogene* **23**, 6292–6298 (2004).
37. Wellbrock, C. *et al.* $^{V599E}$B-RAF is an oncogene in melanocytes. *Cancer Res.* **64**, 2338–2342 (2004).
38. Hingorani, S. R., Jacobetz, M. A., Robertson, G. P., Herlyn, M. & Tuveson, D. A. Suppression of $BRAF^{V599E}$ in human melanoma abrogates transformation. *Cancer Res.* **63**, 5198–5202 (2003).
39. Hoeflich, K. P. *et al.* Oncogenic BRAF is required for tumor growth and maintenance in melanoma models. *Cancer Res.* **66**, 999–1006 (2006).
40. Dankort, D. *et al.* A new mouse model to explore the initiation, progression, and therapy of $BRAF^{V600E}$-induced lung tumors. *Genes Dev.* **21**, 379–384 (2007).
41. Jeong, J. H. *et al.* BRAF activation initiates but does not maintain invasive prostate adenocarcinoma. *PLoS ONE* **3**, e3949 (2008).
42. Dankort, D. *et al.* $Braf^{V600E}$ cooperates with *Pten* loss to induce metastatic melanoma. *Nature Genet.* **41**, 544–552 (2009).
43. Goel, V. K. *et al.* Melanocytic nevus-like hyperplasia and melanoma in transgenic *BRAF*V600E mice. *Oncogene* **28**, 2289–2298 (2009).
44. Chakravarty, D. *et al.* Small-molecule MAPK inhibitors restore radioiodine incorporation in mouse thyroid cancers with conditional BRAF activation. *J. Clin. Invest.* **121**, 4700–4711 (2011).
45. Charles, R. P., Iezza, G., Amendola, E., Dankort, D. & McMahon, M. Mutationally activated BRAFV600E elicits papillary thyroid cancer in the adult mouse. *Cancer Res.* **71**, 3863–3871 (2011).
46. Bollag, G., Freeman, S., Lyons, J. F. & Post, L. E. Raf pathway inhibitors in oncology. *Curr. Opin. Investig. Drugs* **4**, 1436–1441 (2003).
47. Wilhelm, S. M. *et al.* BAY 43-9006 exhibits broad spectrum oral antitumor activity and targets the RAF/MEK/ERK pathway and receptor tyrosine kinases involved in tumor progression and angiogenesis. *Cancer Res.* **64**, 7099–7109 (2004).
48. Kane, R. C. *et al.* Sorafenib for the treatment of advanced renal cell carcinoma. *Clin. Cancer Res.* **12**, 7271–7278 (2006).
49. Kane, R. C. *et al.* Sorafenib for the treatment of unresectable hepatocellular carcinoma. *Oncologist* **14**, 95–100 (2009).
50. Wilhelm, S. *et al.* Discovery and development of sorafenib: a multikinase inhibitor for treating cancer. *Nature Rev. Drug Discov.* **5**, 835–844 (2006).
51. Flaherty, K. T. *et al.* A phase I trial of the oral, multikinase inhibitor sorafenib in combination with carboplatin and paclitaxel. *Clin. Cancer Res.* **14**, 4836–4842 (2008).
52. Hauschild, A. *et al.* Results of a phase III, randomized, placebo-controlled study of sorafenib in combination with carboplatin and paclitaxel as second-line treatment in patients with unresectable stage III or stage IV melanoma. *J. Clin. Oncol.* **27**, 2823–2830 (2009).
53. Ott, P. A. *et al.* A phase II trial of sorafenib in metastatic melanoma with tissue correlates. *PLoS ONE* **5**, e15588 (2010).
54. Wan, P. T. *et al.* Mechanism of activation of the RAF-ERK signaling pathway by oncogenic mutations of B-RAF. *Cell* **116**, 855–867 (2004).
55. Anforth, R. M. *et al.* Cutaneous manifestations of dabrafenib (GSK2118436): a selective inhibitor of mutant BRAF in patients with metastatic melanoma. *Br. J. Dermatol.* 16 Jul 2012 (doi:10.1111/j.1365-2133.2012.11155.x).
56. Falchook, G. S. *et al.* Dabrafenib in patients with melanoma, untreated brain metastases, and other solid tumours: a phase 1 dose-escalation trial. *Lancet* **379**, 1893–1901 (2012).
57. Hauschild, A. *et al.* Dabrafenib in *BRAF*-mutated metastatic melanoma: a multicentre, open-label, phase 3 randomised controlled trial. *Lancet* **380**, 358–365 (2012).
58. Su, Y. *et al.* RAF265 inhibits the growth of advanced human melanoma tumors. *Clin. Cancer Res.* **18**, 2184–2198 (2012).
59. James, J. *et al.* CEP-32496: a novel orally active BRAF(V600E) inhibitor with selective cellular and *in vivo* antitumor activity. *Mol. Cancer Ther.* **11**, 930–941 (2012).

60. Zhang, J., Yang, P. L. & Gray, N. S. Targeting cancer with small molecule kinase inhibitors. *Nature Rev. Cancer* **9**, 28–39 (2009).
61. Fabbro, D., Cowan-Jacob, S. W., Mobitz, H. & Martiny-Baron, G. Targeting cancer with small-molecular-weight kinase inhibitors. *Methods Mol. Biol.* **795**, 1–34 (2012).
62. Tsai, J. *et al.* Discovery of a selective inhibitor of oncogenic B-Raf kinase with potent antimelanoma activity. *Proc. Natl Acad. Sci. USA* **105**, 3041–3046 (2008).
63. Zhang, C. & Bollag, G. Scaffold-based design of kinase inhibitors for cancer therapy. *Curr. Opin. Genet. Dev.* **20**, 79–86 (2010).
64. Hartshorn, M. J. *et al.* Fragment-based lead discovery using X-ray crystallography. *J. Med. Chem.* **48**, 403–413 (2005).
65. Murray, C. W. & Rees, D. C. The rise of fragment-based drug discovery. *Nature Chem.* **1**, 187–192 (2009).
66. Norman, R. A., Toader, D. & Ferguson, A. D. Structural approaches to obtain kinase selectivity. *Trends Pharmacol. Sci.* **33**, 273–278 (2012).
67. Kumar, A. *et al.* Crystal structures of proto-oncogene kinase Pim1: a target of aberrant somatic hypermutations in diffuse large cell lymphoma. *J. Mol. Biol.* **348**, 183–193 (2005).
68. Card, G. L. *et al.* A family of phosphodiesterase inhibitors discovered by cocrystallography and scaffold-based drug design. *Nature Biotech.* **23**, 201–207 (2005).
69. Artis, D. R. *et al.* Scaffold-based discovery of indeglitazar, a PPAR pan-active anti-diabetic agent. *Proc. Natl Acad. Sci. USA* **106**, 262–267 (2009).
70. Bollag, G. *et al.* Clinical efficacy of a RAF inhibitor needs broad target blockade in *BRAF*-mutant melanoma. *Nature* **467**, 596–599 (2010).
**This article details the discovery and development of vemurafenib.**
71. Solit, D. B. *et al. BRAF* mutation predicts sensitivity to MEK inhibition. *Nature* **439**, 358–362 (2006).
**This paper describes the discovery that the *BRAF* oncogene drives the RAF–MEK–ERK pathway in cancer cells.**
72. Halaban, R. *et al.* PLX4032, a selective BRAF(V600E) kinase inhibitor, activates the ERK pathway and enhances cell migration and proliferation of *BRAF* melanoma cells. *Pigment Cell Melanoma Res.* **23**, 190–200 (2010).
73. Joseph, E. W. *et al.* The RAF inhibitor PLX4032 inhibits ERK signaling and tumor cell proliferation in a V600E BRAF-selective manner. *Proc. Natl Acad. Sci. USA* **107**, 14903–14908 (2010).
74. Lee, J. T. *et al.* PLX4032, a potent inhibitor of the B-Raf V600E oncogene, selectively inhibits V600E-positive melanomas. *Pigment Cell Melanoma Res.* **23**, 820–827 (2010).
75. Pratilas, C. A. & Solit, D. B. Targeting the mitogen-activated protein kinase pathway: physiological feedback and drug response. *Clin. Cancer Res.* **16**, 3329–3334 (2010).
76. Sondergaard, J. N. *et al.* Differential sensitivity of melanoma cell lines with *BRAFV600E* mutation to the specific Raf inhibitor PLX4032. *J. Transl. Med.* **8**, 39 (2010).
77. Tap, W. D. *et al.* Pharmacodynamic characterization of the efficacy signals due to selective BRAF inhibition with PLX4032 in malignant melanoma. *Neoplasia* **12**, 637–649 (2010).
78. Yang, H. *et al.* RG7204 (PLX4032), a selective $BRAF^{V600E}$ inhibitor, displays potent antitumor activity in preclinical melanoma models. *Cancer Res.* **70**, 5518–5527 (2010).
79. Sala, E. *et al. BRAF* silencing by short hairpin RNA or chemical blockade by PLX4032 leads to different responses in melanoma and thyroid carcinoma cells. *Mol. Cancer Res.* **6**, 751–759 (2008).
80. Salerno, P. *et al.* Cytostatic activity of adenosine triphosphate-competitive kinase inhibitors in *BRAF* mutant thyroid carcinoma cells. *J. Clin. Endocrinol. Metab.* **95**, 450–455 (2010).
81. Paraiso, K. H. *et al.* Recovery of phospho-ERK activity allows melanoma cells to escape from BRAF inhibitor therapy. *Br. J. Cancer* **102**, 1724–1730 (2010).
82. Shao, Y. & Aplin, A. E. Akt3-mediated resistance to apoptosis in B-RAF-targeted melanoma cells. *Cancer Res.* **70**, 6670–6681 (2010).
83. Basile, K. J., Abel, E. V. & Aplin, A. E. Adaptive upregulation of FOXD3 and resistance to PLX4032/4720-induced cell death in mutant B-RAF melanoma cells. *Oncogene* **31**, 2471–2479 (2011).
84. Deng, W. *et al.* Role and therapeutic potential of PI3K-mTOR signaling in de novo resistance to BRAF inhibition. *Pigment Cell Melanoma Res.* **25**, 248–258 (2012).
85. Kaplan, F. M., Shao, Y., Mayberry, M. M. & Aplin, A. E. Hyperactivation of MEK-ERK1/2 signaling and resistance to apoptosis induced by the oncogenic B-RAF inhibitor, PLX4720, in mutant N-RAS melanoma cells. *Oncogene* **30**, 366–371 (2011).
86. Xing, F. *et al.* Concurrent loss of the PTEN and RB1 tumor suppressors attenuates RAF dependence in melanomas harboring $^{V600E}$*BRAF*. *Oncogene* **31**, 446–457 (2012).
87. Garnett, M. J., Rana, S., Paterson, H., Barford, D. & Marais, R. Wild-type and mutant B-RAF activate C-RAF through distinct mechanisms involving heterodimerization. *Mol. Cell* **20**, 963–969 (2005).
88. Heidorn, S. J. *et al.* Kinase-dead BRAF and oncogenic RAS cooperate to drive tumor progression through CRAF. *Cell* **140**, 209–221 (2010).
89. Yang, H. *et al.* Antitumor activity of BRAF inhibitor vemurafenib in preclinical models of *BRAF*-mutant colorectal cancer. *Cancer Res.* **72**, 779–789 (2012).
90. Rajakulendran, T., Sahmi, M., Lefrancois, M., Sicheri, F. & Therrien, M. A dimerization-dependent mechanism drives RAF catalytic activation. *Nature* **461**, 542–545 (2009).
91. Poulikakos, P. I., Zhang, C., Bollag, G., Shokat, K. M. & Rosen, N. RAF inhibitors transactivate RAF dimers and ERK signalling in cells with wild-type BRAF. *Nature* **464**, 427–430 (2010).
92. Flaherty, K. T. *et al.* Inhibition of mutated, activated BRAF in metastatic melanoma. *N. Engl. J. Med.* **363**, 809–819 (2010).
**This paper reports the results of a Phase I clinical trial that shows the pharmacokinetics and clinical efficacy of vemurafenib.**
93. Kopetz, S. *et al.* PLX4032 in metastatic colorectal cancer patients with mutant BRAF tumors. *J. Clin. Oncol.* **28**, Abstract 3534 (2010).
94. Sosman, J. A. *et al.* Survival in *BRAF* V600-mutant advanced melanoma treated with vemurafenib. *N. Engl. J. Med.* **366**, 707–714 (2012).
**This is a study showing the efficacy of vemurafenib in Phase II clinical trials.**
95. Chapman, P. B. *et al.* Improved survival with vemurafenib in melanoma with BRAF V600E mutation. *N. Engl. J. Med.* **364**, 2507–2516 (2011).
**This is a study showing the efficacy of vemurafenib in Phase III clinical trials.**
96. McArthur, G. A. *et al.* Marked, homogeneous, and early [$^{18}$F]fluorodeoxyglucose-positron emission tomography responses to vemurafenib in *BRAF*-mutant advanced melanoma. *J. Clin. Oncol.* **30**, 1628–1634 (2012).
97. Jiang, C. C. *et al.* Apoptosis of human melanoma cells induced by inhibition of B-$RAF^{V600E}$ involves preferential splicing of bimS. *Cell Death Dis.* **1**, e69 (2010).
98. Nicolaides, T. P. *et al.* Targeted therapy for $BRAF^{V600E}$ malignant astrocytoma. *Clin. Cancer Res.* **17**, 7595–7604 (2011).
99. Esteve-Puig, R., Canals, F., Colome, N., Merlino, G. & Recio, J. A. Uncoupling of the LKB1-AMPKα energy sensor pathway by growth factors and oncogenic $BRAF^{V600E}$. *PLoS ONE* **4**, e4771 (2009).
100. Niehr, F. *et al.* Combination therapy with vemurafenib (PLX4032/RG7204) and metformin in melanoma cell lines with distinct driver mutations. *J. Transl. Med.* **9**, 76 (2011).
101. White, R. M. *et al.* DHODH modulates transcriptional elongation in the neural crest and melanoma. *Nature* **471**, 518–522 (2011).
102. Paraiso, K. H. *et al.* PTEN loss confers BRAF inhibitor resistance to melanoma cells through the suppression of BIM expression. *Cancer Res.* **71**, 2750–2760 (2011).
103. Prahallad, A. *et al.* Unresponsiveness of colon cancer to BRAF(V600E) inhibition through feedback activation of EGFR. *Nature* **483**, 100–103 (2012).
104. Corcoran, R. B. *et al.* EGFR-mediated reactivation of MAPK signaling contributes to insensitivity of *BRAF*-mutant colorectal cancers to RAF inhibition with vemurafenib. *Cancer Discov.* **2**, 227–235 (2012).
105. Montagut, C. *et al.* Elevated CRAF as a potential mechanism of acquired resistance to BRAF inhibition in melanoma. *Cancer Res.* **68**, 4853–4861 (2008).
106. Nazarian, R. *et al.* Melanomas acquire resistance to B-RAF(V600E) inhibition by RTK or N-RAS upregulation. *Nature* **468**, 973–977 (2010).
107. Villanueva, J. *et al.* Acquired resistance to BRAF inhibitors mediated by a RAF kinase switch in melanoma can be overcome by cotargeting MEK and IGF-1R/PI3K. *Cancer Cell* **18**, 683–695 (2010).
108. Shi, H. *et al.* Melanoma whole-exome sequencing identifies $^{V600E}$*B-RAF* amplification-mediated acquired B-RAF inhibitor resistance. *Nature Commun.* **3**, 724 (2012).
109. Little, A. S. *et al.* Amplification of the driving oncogene, *KRAS* or *BRAF*, underpins acquired resistance to MEK1/2 inhibitors in colorectal cancer cells. *Sci. Signal.* **4**, ra17 (2011).
110. Corcoran, R. B. *et al. BRAF* gene amplification can promote acquired resistance to MEK inhibitors in cancer cells harboring the *BRAF* V600E mutation. *Sci. Signal.* **3**, ra84 (2010).
111. Straussman, R. *et al.* Tumour micro-environment elicits innate resistance to RAF inhibitors through HGF secretion. *Nature* **487**, 500–504 (2012).
112. Wilson, T. R. *et al.* Widespread potential for growth-factor-driven resistance to anticancer kinase inhibitors. *Nature* **487**, 505–509 (2012).
113. Solit, D. B. & Rosen, N. Resistance to BRAF inhibition in melanomas. *N. Engl. J. Med.* **364**, 772–774 (2011).
114. Poulikakos, P. I. *et al.* RAF inhibitor resistance is mediated by dimerization of aberrantly spliced BRAF(V600E). *Nature* **480**, 387–390 (2011).
115. Hall-Jackson, C. A. *et al.* Paradoxical activation of Raf by a novel Raf inhibitor. *Chem. Biol.* **6**, 559–568 (1999).
**This paper is the first description of the RAF inhibitor paradox.**
116. Courtois-Cox, S. *et al.* A negative feedback signaling network underlies oncogene-induced senescence. *Cancer Cell* **10**, 459–472 (2006).
117. Dougherty, M. K. *et al.* Regulation of Raf-1 by direct feedback phosphorylation. *Mol. Cell* **17**, 215–224 (2005).
118. Ritt, D. A., Monson, D. M., Specht, S. I. & Morrison, D. K. Impact of feedback phosphorylation and Raf heterodimerization on normal and mutant B-Raf signaling. *Mol. Cell. Biol.* **30**, 806–819 (2010).
119. Hatzivassiliou, G. *et al.* RAF inhibitors prime wild-type RAF to activate the MAPK pathway and enhance growth. *Nature* **464**, 431–435 (2010).
**Together with references 88 and 91, this is one of the key studies that unravels the mechanism of the RAF inhibitor paradox.**
120. Brennan, D. F. *et al.* A Raf-induced allosteric transition of KSR stimulates phosphorylation of MEK. *Nature* **472**, 366–369 (2011).
121. McKay, M. M., Ritt, D. A. & Morrison, D. K. RAF inhibitor-induced KSR1/B-RAF binding and its effects on ERK cascade signaling. *Curr. Biol.* **21**, 563–568 (2011).
122. Hu, J. *et al.* Mutation that blocks ATP binding creates a pseudokinase stabilizing the scaffolding function of kinase suppressor of Ras, CRAF and BRAF. *Proc. Natl Acad. Sci. USA* **108**, 6067–6072 (2011).
123. Su, F. *et al.* RAS mutations in cutaneous squamous-cell carcinomas in patients treated with BRAF inhibitors. *N. Engl. J. Med.* **366**, 207–215 (2012).
**This study documents the occurrence and mechanism of vemurafenib-stimulated cutaneous squamous cell carcinomas.**
124. Oberholzer, P. A. *et al.* RAS mutations are associated with the development of cutaneous squamous cell tumors in patients treated with RAF inhibitors. *J. Clin. Oncol.* **30**, 316–321 (2012).
125. Dietrich, S. *et al.* BRAF inhibition in refractory hairy-cell leukemia. *N. Engl. J. Med.* **366**, 2038–2040 (2012).
126. Gautschi, O. *et al.* A patient with *BRAF* V600E lung adenocarcinoma responding to vemurafenib. *J. Thorac. Oncol.* **7**, e23–e24 (2012).
127. Comin-Anduix, B. *et al.* The oncogenic BRAF kinase inhibitor PLX4032/RG7204 does not affect the viability or function of human lymphocytes across a wide range of concentrations. *Clin. Cancer Res.* **16**, 6040–6048 (2010).
128. Boni, A. *et al.* Selective $BRAF^{V600E}$ inhibition enhances T-cell recognition of melanoma without affecting lymphocyte function. *Cancer Res.* **70**, 5213–5219 (2010).

129. Koch, W. H. Technology platforms for pharmacogenomic diagnostic assays. *Nature Rev. Drug Discov.* **3**, 749–761 (2004).
130. Halait, H. *et al.* Analytical performance of a real-time PCR-based assay for V600 mutations in the *BRAF* gene, used as the companion diagnostic test for the novel BRAF inhibitor vemurafenib in metastatic melanoma. *Diagn. Mol. Pathol.* **21**, 1–8 (2012).
131. Garber, K. Cancer research. Melanoma drug vindicates targeted approach. *Science* **326**, 1619 (2009).
132. Howe, L. R. *et al.* Activation of the MAP kinase pathway by the protein kinase raf. *Cell* **71**, 335–342 (1992).
133. Jamal, S. & Ziff, E. Transactivation of *c-fos* and β-actin genes by *raf* as a step in early response to transmembrane signals. *Nature* **344**, 463–466 (1990).
134. Schubbert, S., Shannon, K. & Bollag, G. Hyperactive Ras in developmental disorders and cancer. *Nature Rev. Cancer* **7**, 295–308 (2007).
135. Warne, P. H., Viciana, P. R. & Downward, J. Direct interaction of Ras and the amino-terminal region of Raf-1 *in vitro*. *Nature* **364**, 352–355 (1993).
136. Leevers, S. J., Paterson, H. F. & Marshall, C. J. Requirement for Ras in Raf activation is overcome by targeting Raf to the plasma membrane. *Nature* **369**, 411–414 (1994).
137. Luo, Z. *et al.* Oligomerization activates c-Raf-1 through a Ras-dependent mechanism. *Nature* **383**, 181–185 (1996).
138. Weber, C. K., Slupsky, J. R., Kalmes, H. A. & Rapp, U. R. Active Ras induces heterodimerization of cRaf and BRaf. *Cancer Res.* **61**, 3595–3598 (2001).

**Acknowledgements**
The authors wish to thank all the employees of Plexxikon who contributed to the work described here. They also thank their colleagues at Roche, the clinical investigators and especially the patients.

**Competing interests statement**
The authors declare competing financial interests: see Web version for details.

**FURTHER INFORMATION**
**ClinicalTrials.gov website:** http://www.clinicaltrials.gov
**ALL LINKS ARE ACTIVE IN THE ONLINE PDF**